

IMPROVED MODELING, DESIGN AND SIMULATION OF GUIDED-WAVE SAW CONVOLVERS

V. M. N. Passaro

Dipartimento di Elettrotecnica ed Elettronica, Politecnico di Bari, ITALY
passaro@poliba.it

Abstract

In this paper a detailed modeling and design of a waveguide surface acoustic wave (SAW) convolver for wide band signal convolution is presented. A number of higher order effects have been taken into account, including SAW triple-transit effect, field confinement in the acoustic waveguide region, SAW Fresnel diffraction, SAW velocity change in the metallized regions, SAW attenuation on the free surface and under the metallized regions, delay temperature coefficient, beam steering effect, and interference due to bulk waves. Numerical results are presented for the correlation of a PSK signal to be used in a CDMA telecommunication system.

Introduction

Code division multiple access (CDMA) telecommunication wireless systems, indoor/outdoor spread-spectrum wireless for packet-data and packet-voice communications and other analogous, more complicated systems such as the code-time division multiple access (CTDMA) [1], require the autocorrelation between high frequency signals in order to extract the coded information with appropriate filtering. This operation can be carried out with high resolution, broad bandwidth, large processing gain, small size and low loss in surface acoustic wave (SAW) convolvers. These components allow an improved performance against multipath interference, are suited to indoor spread-spectrum communications in buildings with highly-reflecting structures, and usually give good jamming protection. They are based on the interaction of two counter-propagating acoustic waves, induced by piezoelectric transducers in ferroelectric materials (such as Z-propagating Y-cut lithium niobate), and used to obtain the required autocorrelation function under a parametric centre electrode. The output signal is extracted as voltage of the centre electrode. Then, the SAW convolver behaves as a programmable linear filter. A number of papers have been recently presented for the analysis and design of such device. Here a general model which can take into account several second order effects which decrease the device performance, allowing a number of significant improvements to be used for design purposes.

In the analysis presented in this paper, these higher order effects have been accurately considered, including the triple-transit effect, which induces at the output of the device the overlapping of undesired echoes on the useful signal, and the reflectivity of the

parametric plate, calculated on the basis of the reflective array modeling approach [2]. Moreover, all the main second-order perturbation effects have been taken into account, including the SAW Fresnel diffraction, SAW velocity change in the metallized regions, SAW attenuation on the free surface and under the metallized regions, delay temperature coefficient, beam steering effect, interference due to bulk waves, and so on. In the paper, the improved modeling and a number of numerical simulations, particularly useful in CTDMA systems, are presented to show the SAW convolver performance.

Modeling

A scheme of SAW convolver with focused interdigitated transducers (FIDT) is shown in the next Fig. 1:

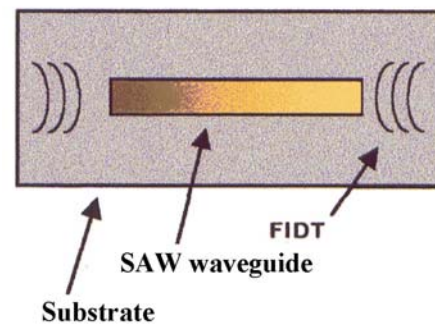


Figure 1 : SAW convolver with FIDT.

The centre parametric plate (SAW waveguide) performs the correlation integral between the two input signals applied on the FIDTs. Instead of focused IDT, two beam width compressors (BWC) can be used to match the different SAW widths. Since the centre electrode acts as a monomodal metallic waveguide for SAWs traveling along the device, this architecture is known as degenerate waveguide convolver. Acoustic diffraction considerations require that the IDT electrode width w is large enough, while the acoustic wave monomodal condition determines the width a of the centre plate electrode. The required integration time defines the plate length L . The main disadvantage of this device consists in the presence of a number of interference signals generated by multiple reflections due to acoustic impedance mismatch between the electrodes and the centre plate.

If we apply two electrical signals, $S(t)$ and $R(t)$, to the interdigitated transducers, two counter-propagating SAWs are excited. When the SAW power flow is high

enough, larger than 10 mW/mm, the nonlinear behaviour of the material becomes significant, producing a number of quadratic terms, among which the correlation function between $S(t)$ and $R(t)$. It is a standing wave, which can be easily detected by the centre metallic plate on the substrate surface. The signal measured at the output can be so described:

$$2 \cos(2\omega_0 t) \int_0^L S\left(t - \frac{z}{v}\right) \cdot R\left(t + \frac{z}{v}\right) dz \quad (1)$$

because the metallic plate works as an integrator. It can be noted that the convolution product is multiplied by a sinusoidal signal at $2\omega_0$, this means that the output signal is obtained at doubled frequency with respect to the input signal mid-band frequency. However, a number of interference signals are generated by multiple reflections due to acoustic impedance mismatch of electrodes and centre plate. These noise contributions have been considered in the general quadratic formulation of Eqn.(1), as:

$$\int \left[c(a_r(t, z) + a_s(t, z)) + c_{NL}(a_r(t, z) + a_s(t, z))^2 + \dots \right] dz \quad (2)$$

In order to evaluate the mismatching due to interdigitated electrodes, the Mason equivalent model has been used. If we consider a propagating SAW, an acoustic impedance can be defined as $Z_0 = F/v$ and an electrical impedance as $Z_e = Z_0/\phi^2$, being ϕ a transformation constant. In the presence of a metallic stripe on the crystal surface, the relevant change of acoustic impedance causes the reflection of incident acoustic wave with reflection coefficient (from medium i to medium j) given by:

$$\rho_{ij} = -\rho_{ji} = \frac{Z_j - Z_i}{Z_j + Z_i}$$

where Z_i and Z_j are the impedances of regions i and j , respectively. The mechanism of multiple reflections between IDT regions and centre electrode is described by the model of Fig. 2, where a number of reflection and transmission coefficients have been defined, together with the relevant phase changes:

- $\rho_{45} = |\rho_{45}(\omega)| \exp[j\phi_{45}(\omega)]$
- $\rho_{21} = |\rho_{21}(\omega)| \exp[j\phi_{21}(\omega)]$
- $\rho_{32} = \rho_{34} = |\rho(\omega)| \exp[j\phi(\omega)]$
- $\rho_{23} = \rho_{43} = |\rho(\omega)| \exp[j\phi(\omega) + j\pi]$
- $t_{32} = t_{34} = |1 - \rho(\omega)| \exp[j\theta(\omega)]$
- $t_{23} = t_{43} = |1 + \rho(\omega)| \exp[j\alpha(\omega)]$

The SAWs are represented by $A \cos(\omega_0 t - \beta z)$ and $B \cos(\omega_0 t + \beta z)$, as driven by signals $S(t)$ and $R(t)$,

respectively, where $\beta = 2\pi/\lambda$ is the acoustic wavenumber.

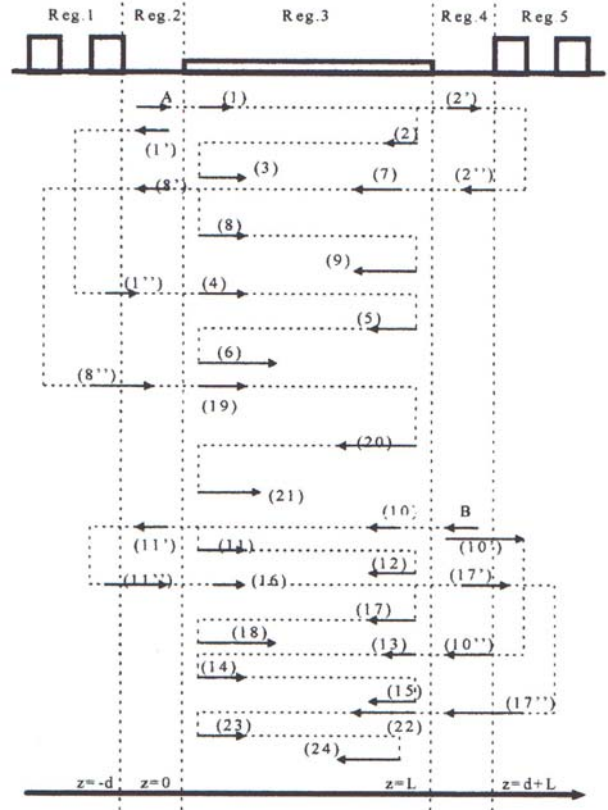


Figure 2 : Convolver multiple reflections.

The following assumptions in the model have been made:

- Equal distance between the centre metallic plate and the input IDTs, d ;
- Second-order electro-optic effect negligible: this means that the acoustic impedance does not depend on the acoustic power, and it is justified at low power levels;
- Independent reflections and distortions of the two main SAWs: this assumption means to use the superposition principle and it is practical good quality crystals are used;
- Since the metallic plate is usually several thousands of acoustic wavelengths long, the contributions due to traveling-wave terms are assumed negligible with respect to the standing-wave ones;
- The difference between the SAW propagation constants of metallized and free surfaces, β and β^* , respectively, has been considered. In fact, the reflections at the interfaces between different media depend on this difference, too.

Therefore, the contributions due to both signals are nine waves, i.e. $A_i \cos(\omega_0 t + \psi_i)$, $i=1,2,\dots,9$, three waves $A_j \cos(\omega_0 t + \psi_j)$, $j=1,2,3$, nine waves $A_k \cos(\omega_0 t + \psi_k)$, $k=10,11,\dots,18$, and three waves $A_l \cos(\omega_0 t + \psi_l)$, $l=22,23,24$. Then, a total of 24 SAW

waves has been considered. Now, the correlation term has been calculated by the squared sum of all the SAW contributions, as depicted in Eqn. (2). Therefore, by using the trigonometric identities, the general expression of the correlation function has been obtained as:

$$2 \sum_{i=1}^{24} \left[\sum_{j=i+1}^{24} A_j \cos(\alpha_j t + \psi_j) \cdot A_i \cos(\alpha_i t + \psi_i) \right] = \sum_{i=1}^{23} \left\{ \sum_{j=i+1}^{23} A_i A_j \left[\cos(\psi_i - \psi_j) + \cos(2\alpha_j t + \psi_i + \psi_j) \right] \right\} \quad (3)$$

Among all the SAW contributions, a number of them can be neglected with respect to the others under the triple-transit suppression (TTS) assumption. Then, the integral contribution terms, which are taken into account in order to evaluate the signal at the output of the SAW convolver, are calculated by the interaction of the wave pairs (10,11), (1,13), (4,10), (1,5), (1,7), (2,4), (10,14), (10,16), (11,13) and (1,10). The couple (1,10) represents the desired convolution signal.

Design and simulation

Two uniform IDTs without apodization have been considered, since not critical frequency requirements were assumed. Once the substrate material is chosen and input data, IF center frequency, $f=140$ MHz ($\lambda = 24 \mu\text{m}$), bandwidth and signal type are given, the design procedure of IDT is carried out under matching load (50Ω) and acoustic diffraction free conditions. Then, all the design parameters have been found, including the parametric electrode width (optimal value $a = 84 \mu\text{m}$ to assure the monomodal condition), the curvature radius of focused transducer R , the transducer aperture width ($w = 316 \mu\text{m}$), the parametric electrode length ($L = 44$ mm), the IDT number of periods ($N_p = 4$), the SAW attenuation $\alpha = 0.0476 \text{ dB}/\mu\text{s} = 0.778 \text{ dB}$ ($f = 140$ MHz) for a convolver total length of 56 mm. The SAW dispersion in metallized regions is $v = v_m(1 - 0.287T/\lambda)$, where T is the Al electrode thickness, the calculated resistance and capacitance of parametric electrode are $R = 69.67 \Omega$ and $C = 5.67 \text{ pF}$, respectively, the power loss on external load with respect to the open circuit voltage is $\eta_o = 0.19$.

The bilinear factor is $C_{NL} = 10 \log[P_{out}/(P_{in1}P_{in2})] = 10 \log(\eta_o M^2 Q^2 \eta_{con}^2 / 2R_L)$, where η_{con} is the electro-mechanical conversion efficiency, $Q = P_{par}/(aP_{tot})$ is the convolver figure of merit, P_{par} is the acoustic power guided under the parametric electrode and P_{tot} is the total acoustic power launched by the transducer. The reflection coefficient of the parametric electrode

$\rho_{par} = 0.35Tf/v (= 0.0028 \text{ at } 140 \text{ MHz})$ has been used.

The parametric electrode has been designed under the monomodal condition by solving the acoustic wave equation in the confined structure. The following values have been used: LiNbO₃ substrate anisotropic factor $b = 0.25$; SAW velocity of YZ-LiNbO₃ substrate, $v = 3488 \text{ m/s}$; SAW velocity change (YZ - LiNbO₃) in metallized regions (v_m) $\Delta v/v = (v_m - v)/v = 0.0241$; characteristic factor of YZ-LiNbO₃ substrate, $M = 1.2 \cdot 10^{-4} \text{ V m/W}$; load resistance of parametric electrode $R_L = 50 \Omega$; $\eta_{con} = 0.1$.

Fig. 3 shows the figure of merit Q versus a , for different values of the R/w ratio. If $a = 84 \mu\text{m}$ and $T = 0.2 \mu\text{m}$ are assumed, the best Q is obtained for $R/w = 9.49$, i.e. the FIDT radius is $R \approx 3$ mm. In this case, a high power transfer efficiency from transducer to parametric electrode can be obtained, $\eta_p = 88.5\%$.

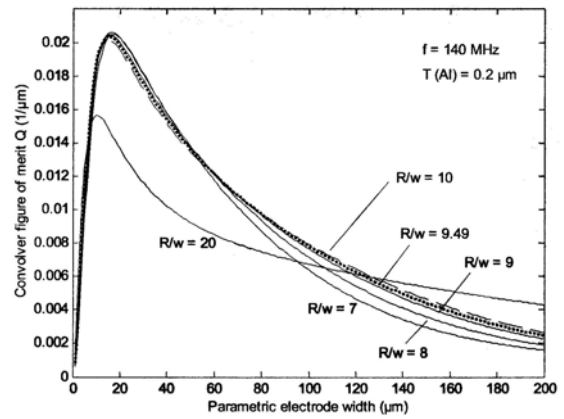


Figure 3 : Q versus a , changing R/w .

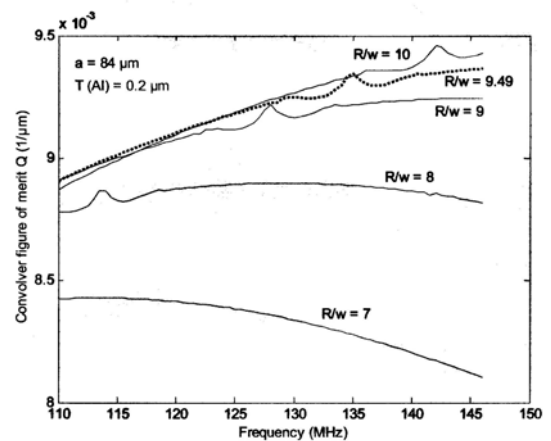


Figure 4 : Q versus f , changing R/w .

In Fig. 4 Q is sketched as a function of the signal frequency. A slight increase of the curve around $f = 140$ MHz for $R/w = 9.49$ can be noted, without any significant influence on the output power.

The value of the power bilinear factor is $C_{NL} = -46.2$ dBm (amplitude factor $c_{NL} = 0.0049$) for $a = 84 \mu\text{m}$ and $R/w = 9.49$.

A software program has been written and tested for the simulation of the SAW device. The above summarized integrals of the model are evaluated with a relative error of 10^{-4} . The convolver has been simulated in degenerate mode (equal inputs) at $f = 140$ MHz. The first simulation uses as input signals a finite rectangular pulse $1 \mu\text{s}$ long: the results are shown in Figs. 5-6, where the triple transit effect as a function of time (μs), and the triple transit spectrum are given, respectively.

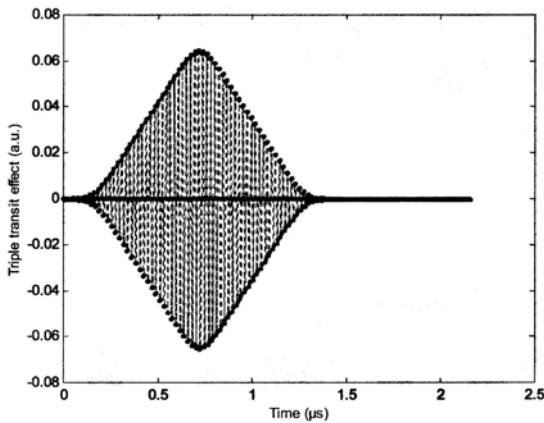


Figure 5 : Triple-transit signal versus time.

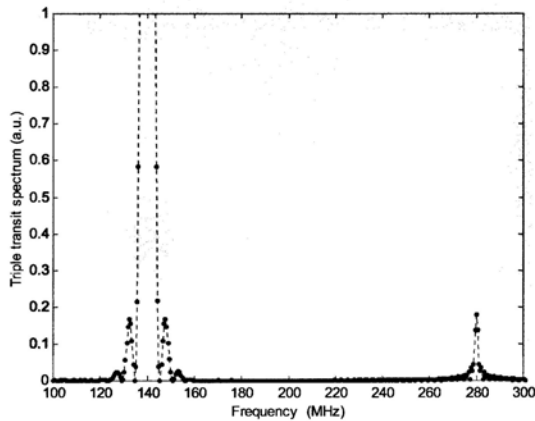


Figure 6 : Triple transit spectrum.

The signal/noise ratio (SNR) calculated over 70 MHz around 280 MHz is equal to 67.67 dB, while the SNR calculated at 280 MHz is 77.14 dB. The signal side lobe suppression is -29.7 dB. From Fig. 6, the ratio of maxima at 140 and 280 MHz is 28.5.

In the second simulation, a PSK signal with 13 bit Barker code (0101001100000) has been assumed, $0.41 \mu\text{s}$ long. Figs. 7-8 show the results of simulation. The signal/noise ratio (SNR) calculated over 70 MHz around 280 MHz is 52.98 dB.

The SNR calculated at 280 MHz is 82.1 dB. The signal side lobe suppression is -34.17 dB and the 3dB signal bandwidth is 3.4 MHz.

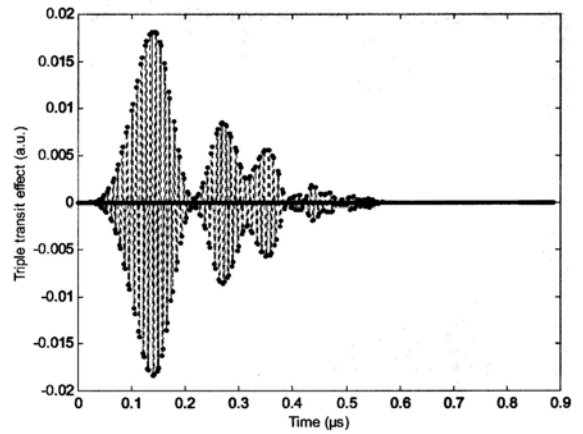


Figure 7 : Triple transit effect versus time.

From Fig. 8, the ratio of maxima at 140 and 280 MHz is 50.7, much better than in the first case.

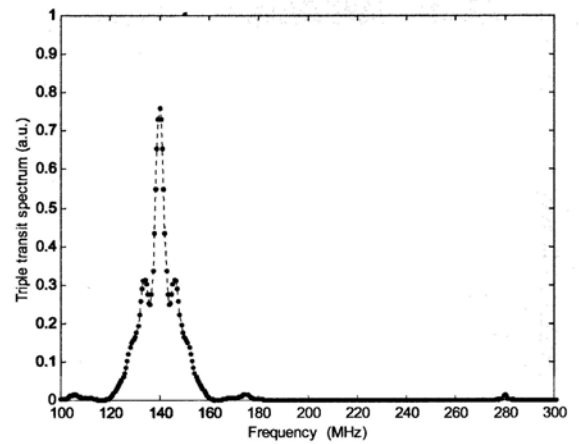


Figure 8 : Triple transit spectrum.

Values of SNR as large as 80 dB with bilinear factors better than -40 dBm well demonstrate the high potential of these devices, in very good agreement with experimental results presented in literature.

Conclusions

An accurate modeling and design procedure of a degenerate waveguide SAW convolver has been presented to be used for autocorrelation functions in highly selective wireless systems, such as CDMA or CTDMA.

References

- [1] V.M.N. Passaro, M.N. Armenise, V.V. Proklov et al., "Development of Mobile Communication Systems on Solid State Elementary Basis (DMCSSSEB)", COP 959 European Project, Final Report, pp. 1-109, Bruxelles, 10 April 1999.
- [2] D. P. Morgan, "Reflective array modeling for reflective and directional SAW transducers", IEEE Trans. on Ultrasonics, Ferroel. and Fr. Control, vol. 45, pp. 152-157, 1998.